REPORT DOCUMENTATION PAGE

Form Approved
OMB No. 0704-0188

1. REPORT DATE *(DD-MM-YYYY)*	2. REPORT TYPE	3. DATES COVERED *(From - To)*
08-05-1997	Journal Article	1 Oct 96 - 30 Sept 00

4. TITLE AND SUBTITLE
OBSERVATION OF QUANTUM-CONFINED STARK EFFECT IN TRIPLE-COUPLED INGAAS/GAAS/ALGAAS QUANTUM WELL INFRARED PHOTODETECTOR

5a. CONTRACT NUMBER

5b. GRANT NUMBER

5c. PROGRAM ELEMENT NUMBER
61102F

6. AUTHOR(S)
Sheng S. Li, J. C. Chiang, A. Singh, and M. Z. Tidrow

5d. PROJECT NUMBER
2305

5e. TASK NUMBER
TJ

5f. WORK UNIT NUMBER
02

7. PERFORMING ORGANIZATION NAME(S) AND ADDRESS(ES)
Air Force Research Laboratory
3550 Aberdeen Ave. SE
Kirtland AFB, NM 87117-5776

8. PERFORMING ORGANIZATION REPORT NUMBER

9. SPONSORING / MONITORING AGENCY NAME(S) AND ADDRESS(ES)

10. SPONSOR/MONITOR'S ACRONYM(S)

11. SPONSOR/MONITOR'S REPORT NUMBER(S)

12. DISTRIBUTION / AVAILABILITY STATEMENT
Approved for Public Release; Distribution is Unlimited.

13. SUPPLEMENTARY NOTES

14. ABSTRACT
We have investigated the quantum-confined Stark effect (QCSE) in several n-type InGaAs/GaAs/AlGaAs triple-coupled quantum well infrared photodetectors (TC-QWIPs) for 8-12 μm long wavelength infrared (LWIR) detection. The basic structure of this TC-QWIP consists of three coupled quantum wells (QWs) formed by a Si-doped $In_xGa_{1-x}As$ QW and two undoped thin GaAs QWs separated by two thin $Al_yGa_{1-y}As$ barriers. Three TC-QWIP devices with varying indium and aluminum compositions were fabricated and characterized. A strong QCSE for the ($E_1 \rightarrow E_3$) transition was observed in the wavelength range of 8.2 - 9.1 μm, 10.8 - 11.5 μm, and 9.4 - 10.7 μm for QWIP-A, -B, and -C, respectively. These devices exhibit a linear dependence of peak wavelength on the applied bias voltage over these wavelengths ranges. Peak responsivities, R_1 = 0.05, 0.33 A/W and detectivities, $D^*_{BLIP} = 6.1x10^9$, $1.63x10^{10}$cm-$Hz^{1/2}$/W at V_b=5, 4 V, λ_p=8.6, 11.2 μm, and T_{BLIP}=66, 50 K were obtained for QWIP-A and -B, respectively. For QWIP-C, R_1=0.19 A/W was obtained at λ_p=9.3 μm, V_b=7 V, and T+60 K.

15. SUBJECT TERMS
Triple-coupled, photodetectors, three-coupled, quantum wells, indium, aluminum composites

16. SECURITY CLASSIFICATION OF:			17. LIMITATION OF ABSTRACT	18. NUMBER OF PAGES	19a. NAME OF RESPONSIBLE PERSON
a. REPORT	b. ABSTRACT	c. THIS PAGE			David Cardimona
Unclassified	Unclassified	Unclassified	Unlimited	15	19b. TELEPHONE NUMBER *(include area code)* (505) 846-5807

Standard Form 298 (Rev. 8-98)
Prescribed by ANSI Std. 239.18

OBSERVATION OF QUANTUM-CONFINED STARK EFFECT IN TRIPLE-COUPLED INGAAS/GAAS/ALGAAS QUANTUM WELL INFRARED PHOTODETECTOR

Sheng S. Li[a], J. C. Chiang[a], A. Singh[b], and M. Z. Tidrow[c]

a. Dept. of Electrical and Computer Engineering, University of Florida
Gainesville, FL 32611

b. Phillips Laboratory, PL/VTMR,
Kirtland AFB, NM 87117

c. Army Research Laboratory, AMSRL-SE-EM,
Adelphi, MD 20783

ABSTRACT

We have investigated the quantum-confined Stark effect (QCSE) in several n-type InGaAs/GaAs/AlGaAs triple-coupled quantum well infrared photodetectors(TC-QWIPs) for 8-12 μm long wavelength infrared (LWIR) detection. The basic structure of this TC-QWIP consists of three coupled quantum wells (QWs) formed by a Si-doped $In_xGa_{1-x}As$ QW and two undoped thin GaAs QWs separated by two thin $Al_yGa_{1-y}As$ barriers. Three TC-QWIP devices with varying indium and aluminum compositions were fabricated and characterized. A strong QCSE for the $(E_1 \rightarrow E_3)$ transition was observed in the wavelength range of 8.2 – 9.1 μm, 10.8 – 11.5 μm, and 9.4 – 10.7 μm for QWIP-A, -B, and -C, respectively. These devices exhibit a linear dependence of peak wavelength on the applied bias voltage over these wavelength ranges. Peak responsivities, R_i = 0.05, 0.33 A/W and detectivities, $D^*_{BLIP} = 6.1\times10^9$, 1.63×10^{10} cm-Hz$^{1/2}$/W at V_b = 5, 4 V, λ_p = 8.6, 11.2 μm, and T_{BLIP} = 66, 50 K were obtained for QWIP-A and -B, respectively. For QWIP-C, R_i = 0.19 A/W was obtained at λ_p = 9.3 μm, V_b = 7 V, and T = 60 K.

INTRODUCTION

Recently, there have been reports[1,2] on the study of a triple-coupled quantum well infrared photodetector (TC-QWIP) based on InGaAs/GaAs/AlGaAs material system for 8-12 μm long wavelength infrared (LWIR) detection. Using bandgap engineering, a wide variety of multicolor QWIPs such as voltage-tunable coupled QWIPs and two-stack two-color QWIPs for detection in both MWIR and LWIR bands have been published.[3-9] Tidrow et al.[5] have reported a two-coupled asymmetrical QWIP for three-color LWIR detection. However, the Stark shift effect was small with this two-well coupling structure. Huang and Lien[1] proposed a two-depth three-coupled quantum well (TCQW) for a voltage tunable IR detector application. Based on their theoretical calculations, they predicted a very large Stark shift effect with wavelength tunability in the 8 to 14 μm range by an applied bias voltage to the two-depth TCQW structure. This wavelength tunability is highly desirable for IR imaging applications such as target discrimination and identification. The first demonstration of wavelength tunability was reported recently by Chiang et al.[2] using the triple-coupled InGaAs/AlGaAs/GaAs quantum well structures. The mechanism of the quantum-confined Stark effect (QCSE) has been presented by Bastard et al.[10] to describe the eigenenergy shift in optical absorption in an isolated-quantum-well structure subject to an electric field perpendicular to the epitaxial layers. At weak fields a quadratic Stark shift is found whose magnitude depends strongly on the well width. Besides, in the TCQW structures, there is another field-induced Stark effect which will also enhance the blue shift in optical absorption. It can be approximated as the potential drop between the centers of the TCQWs. Therefore a linear dependence of the energy separation on the perpendicular electric field is expected. In this paper we report a detailed study of three voltage-tunable triple-coupled quantum well infrared photodetectors (TC-QWIPs) using InGaAs/GaAs/AlGaAs grown on GaAs for the 8 – 12 μm detection.

GROWTH AND FABRICATION OF TC-QWIPS

The basic structure of the TC-QWIP is composed of a three-coupled quantum wells (TCQWs) separated by two thin $Al_yGa_{1-y}As$ barrier layers. QWIP-A, and -B each with twenty repeats of the TCQWs sandwiched between the 50 nm $Al_yGa_{1-y}As$ barrier layers were grown on the semi-insulating GaAs substrate by using molecular beam epitaxy technique. The TCQW consists of a Si-doped (5×10^{17} cm^{-3}) $In_xGa_{1-x}As$ deep well (x = 0.06, 0.03 and width = 6, 8 nm for QWIP-A and -B, respectively) and two undoped GaAs shallow wells (width = 3, 3.5 nm for the left, middle well) separated by two 1.6 nm $Al_yGa_{1-y}As$ thin barriers (y = 0.21 and 0.19 for QWIP- A and B, respectively). Heavily doped GaAs cap layers were grown on the top and bottom of the TCQWs for ohmic

contacts. For QWIP-C, 20 periods of TCQWs were used with $In_xGa_{1-x}As$ (x = 0.05) QWs doped to 5×10^{17} cm^{-3}, while other layer structures and device parameters are similar to QWIP-A and -B. A mesa structure with an active area of 200×200 μm^2 was created in the TC-QWIPs by wet chemical etching to facilitate for the device characterization. A square contact ring composed of AuGe/Ni/Au was first deposited around the periphery of the mesa and alloyed for ohmic contacts. The devices were then processed with a 45° polished facet for coupling IR radiation.

RESULTS AND DISCUSSION

Quantum-Confined Stark Effect (QCSE)

Figure 1(a) shows the schematic diagram of the conduction band and the bound state energy levels for an isolated three-QWs structure, and Fig.1(b) is for a TC-QWIP under positive bias condition. For the TC-QWIP, due to the strong coupling effect of the three asymmetrical QWs and two thin AlGaAs barriers, the bound states in the GaAs QWs and the first excited state in the InGaAs QW are coupled to form the second (E_2) and third (E_3) bound states inside the TCQWs under applied bias condition, as illustrated in Fig.1(b). The intersubband transition for the TC-QWIP is dominated by the bound-to-bound transition between the E_1 and E_3 states, while two secondary photoresponse peaks due to E_1 to E_2 and E_1 to E_C states transitions were also observed in QWIP-A under large and reverse bias conditions. To calculate the energy levels in the TCQWs, the effects of electron-electron interaction[11] and strain-induced energy shift[12] in the $In_xGa_{1-x}As$ quantum well were considered. Using multilayer transfer matrix method (TMM), the envelope wave functions and the energy levels of the bound states and continuum states were calculated. Figure 2(a) and 2(b) show the calculated envelope wave functions, ϕ_1 and ϕ_3, of QWIP-A under zero bias and V_b = 7.5 V, respectively. Figure 3(a), 3(b), and 3(c) show the calculated transmission coefficients of QWIP-A, -B, and -C, respectively. The results show that there are three bound states formed in the TCQWs. The calculated values of the conduction band offset (ΔE_C = 212, 163, and 200 meV) were found in excellent agreement with the measured values (ΔE_C = 220, 165, and 205 meV) determined from the activation energy of the dark current versus inverse temperature plot at low bias for QWIP-A, -B, and -C, respectively. Figure 4(a), 4(b), and 4(c) show the calculated energy spacing ΔE_{13} for intersubband absorption and the subband energies E_1 and E_3 as a function of the applied bias voltage for QWIP-A, -B, and -C, respectively. The solid lines are the calculated values while solid squares denote the measured values. Good agreement between the theoretical calculations and the experimental data were obtained. Both the subband energies E_1 and E_3 increase linearly with the applied bias, but E_3 increases faster with V_b than that of E_1, indicating a larger QCSE for the E_3 level. As a result of the

linear dependence of energy spacing ΔE_{13} with applied bias for the intersubband absorption, a linear wavelength tunability with the applied voltage can be readily achieved in a TC-QWIP .

Photoresponse Measurements

The spectral responsivity curves of QWIP-A, -B, and -C were measured as a function of temperature and bias voltage using a 0.25 m grating monochromator with a calibrated blackbody source (T_b = 1000 °C). The responsivities were found to be nearly independent of temperature up to 77 K.

QWIP-A. Fig.5(a) shows the plot of responsivity versus wavelength for QWIP-A under different bias conditions. For QWIP-A, three response peaks at 11.5 μm, 8.2 - 9.1 μm, and 7.2 μm were observed under different positive and negative bias voltages, which are attributed to the transitions from the ground state to the first and second excited states, and the continuum states, respectively. The main detection peak due ($E_1 \rightarrow E_3$) transition was observed for $V_b > 2.5$V. A spectral responsivity of 0.06 A/W was obtained at V_b = 5V and λ_p = 8.6 μm. The low responsivity for this QWIP was attributed to the poor quality of this wafer growth. A linear dependence of the peak detection wavelength with applied bias voltage was obtained for the ($E_1 \rightarrow E_3$) intersubband transition, as shown in Fig.6(a). The blue shift for the ($E_1 \rightarrow E_3$) transition is a direct result of the increase in energy spacing, ΔE_{13}, with the applied bias voltage (QCS effect), with detection peak shifting to shorter wavelength. The tunable wavelength range for the ($E_1 \rightarrow E_3$) transition was found to be from 8.2 to 9.1 μm, and the BLIP detectivity, D^*_{BLIP}, was found to be 6.1×10^9 cm-Hz$^{1/2}$/W at V_b = 5 V, λ_p = 8.6 μm, FOV 180° and T_{BLIP} = 66 K, using a calculated photoconductive gain of g = 0.77 from the noise model of Wang et al.[13] In addition, another photoresponse peak due to ($E_1 \rightarrow E_2$) transition was also observed at V_b = 6 V (see Fig.5a). However, under negative bias condition, only one response peak at λ_p = 7.2 μm was observed at V_b =
-5.5 V, which was attributed to the bound-to-continuum states ($E_1 \rightarrow E_c$) transition.

QWIP-B. Fig.5(b) shows the responsivity versus wavelength for QWIP-B; only two response peaks due to ($E_1 \rightarrow E_3$) and ($E_1 \rightarrow E_C$) transitions were observed in the wavelength range of 6.5 -13 μm under positive bias condition. The main detection peak is due ($E_1 \rightarrow E_3$) transition, which also shows a strong QCS effect in this device, while photoresponse due to ($E_1 \rightarrow E_2$) transition (λ_p > 14 μm) was not studied in this work.

The responsivity was found to be 0.41 A/W at λ_p = 10.8 μm and V_b = 5V. This is an order of magnitude higher than that of QWIP-A for the ($E_1 \rightarrow E_3$) transition at λ_p = 8.6 μm . QWIP-B also exhibits a linear dependence of the peak detection wavelength on the applied bias voltage, as illustrated in Fig.6(b). The tunable wavelengths for the ($E_1 \rightarrow E_3$) transition were found to be in the range of 10.8 -11.5 μm. A maximum BLIP detectivity, D^*_{BLIP}, of 1.63x10^{10} cm-Hz$^{1/2}$/W at V_b = 4 V, λ_p = 11.2 μm, FOV of 180° and T_{BLIP} = 50 K was obtained, using a calculated photoconductive gain of g = 0.6.[13]

QWIP-C. The responsivity versus wavelength curves for QWIP-C are shown in Fig.5(c). The results show one main response peak due to ($E_1 \rightarrow E_3$) transition under positive bias with response peak wavelengths varying from 10.7 to 9.4 μm when bias voltages vary from 0 to 7 V. The responsivity was found to be 0.19 A/W at λ_p = 9.3 μm and V_b = 7 V. Under negative bias condition, a response peak due to ($E_1 \rightarrow E_C$) transition was observed at λ_p = 8.2 μm and V_b = -5 V (not shown in Fig.5(c)). A linear dependence of the peak wavelength on the bias voltage was also found in QWIP-C as shown in Fig.6(c), revealing the voltage tunability for the TC-QWIPs.

From the results discussed above, it is noted that the main detection peak for all three TC-QWIPs reported here is dominated by the ($E_1 \rightarrow E_3$) intersubband transition, while photoresponse due ($E_1 \rightarrow E_2$) transition can only be observed at higher positive bias condition. Another response peak at a shorter wavelength can be found when a negative bias is applied to these TC-QWIPs. The tunable detection wavelengths were found to be in the 8 to 12 μm range under positive bias condition. In contrast to the prediction given in Ref.(1), no Stark shift effect was observed under negative bias condition for these devices. The tunable wavelength range for QWIP-A was also found to be smaller than that predicted by Huang and Lien[1], which used the similar device parameters as QWIP-A in their calculations. One possible explanation could be attributed to the fact that they neglected the electron-electron interaction and the strain effects in the band offset calculations. From our calculations, the actual band offset for QWIP-A was smaller (ΔE_C = 212 meV) than the 250 meV given in Ref. (1). Thus, the tunable wavelength range is expected to be smaller than that predicted by Ref. (1) when both the electron-electron interaction and strain effects are considered in the InGaAs quantum well.

I-V Measurements

The dark current density versus bias voltage curves measured at T = 31 K to 77 K for QWIP-A, -B, and -C are shown in Figs.7(a), 7(b), and 7(c), respectively. These devices show the asymmetrical dark current-voltage characteristics under positive and negative

bias conditions, which is attributed to the asymmetrical potential barriers in the TCQW structure. Since the effective barrier height under negative bias is smaller than that of the positive bias case, J_d is larger under negative bias than the positive bias condition. It is also noted that J_d for QWIP-A is much smaller than those of QWIP-B and -C due to the larger conduction band offset and shorter cutoff wavelength for the former. For comparison, the 300 K background photocurrent density curves (with a 180° FOV) are also included in Figs.7(a), (b), and (c) for QWIP-A, -B, and -C, respectively. The devices are under background limited performance (BLIP) for $T \leq 66$ K, $V_b \leq 7$ V, $T \leq 50$ K, $V_b \leq 5$ V, and $T \leq 60$ K, $V_b \leq 6$ V for QWIP-A, -B, and -C, respectively.

CONCLUSIONS

In conclusion, we have investigated the quantum confined Stark (QCS) effect in the triple-coupled n-type InGaAs/GaAs/AlGaAs quantum well infrared photodetectors (TC-QWIPs). Three TC-QWIPs (QWIP-A, -B, and -C) with different quantum well and barrier compositions have been fabricated and analyzed. Using QCS shift effect, the wavelength tunability by the applied bias voltage in the wavelength range of 8 -12 μm has been demonstrated for these TC-QWIPs. Several photoresponse peaks in the LWIR waveband have been observed in these QWIPs under different bias conditions. Further optimization of TC-QWIP structure will enable the fabrication of highly sensitive and low cost QWIPs for LWIR imaging array applications.

ACKNOWLEDGEMENTS

This work was sponsored and monitored by the US Air Force Material Command, Phillips Laboratory/VTMR, Kirtland AFB, NM, under a subcontract with Maxwell Technology Inc., Dr. James Duffy is the program manager and Lt. Ann Marie Shover is the contract monitor at PL/VTMR. The authors would like to thank Prof. C. P. Lee of National Chiao Tung University in Taiwan for MBE growth of QWIP-A, Dr. Pin Ho of Lockheed-Martin for growing QWIP-B. QWIP-C sample was grown by Quantum Epitaxy Design Inc.

REFERENCES

1. Y. Huang and C. Lien, J. Appl. Phys., **77**, 3433 (1995).
2. J. C. Chiang, S. S. Li, M. Z. Tidrow, P. Ho, M. Tsai, C. P. Lee, Appl. Phys. Lett., **69**, 2412 (1996).
3. B. F. Levine, J. Appl. Phys., **74**, R1 (1993).
4. H. C. Liu, J. Li, J. R. Thompson, Z. R. Wasilewski, M. Buchanan, and J. G. Simmons, IEEE Electron Devices Lett., **14**, 556 (1993).
5. M. Z. Tidrow, K. K. Choi, C. Y. Lee, W. H. Chang, F. J. Towner, and H. R. Chen, Appl. Phys. Lett., **64**, 1268 (1994).
6. K. L. Tsai, K. H. Chang, C. P. Lee, K. F. Huang, J. S. Tsang, and H. R. Chen, Appl. Phys. Lett., **62**, 3504 (1993).
7. Y. H. Wang, J. C. Chiang, S. S. Li, and P. Ho, J. Appl. Phys., **76**, 2538 (1994).
8. M. Z. Tidrow, K. K. Choi, A. J. DeAnni, W. H. Chang, and S. P. Svensson, Appl. Phys. Lett., **67**, 1800 (1995).
9. C. J. Chen, K. K. Choi, M. Z. Tidrow, and D. C. Tsui, Appl. Phys. Lett., **68**, 1446 (1996).
10. G. Bastard, E. E. Mendez, L. L. Chang, and L. Esaki, Phys. Rev., **B28**, 3241 (1983).
11. J. W. Choe, O. Byungsung, K. M. S. V. Bandara, and D. D. Coon, Appl. Phys. Lett., **56**, 1679 (1990).
12. G. E. Bir and G. E. Pikus, Symmetry and Strain-Induced Effects in Semiconductors, Wiley, New York (1974).
13. D. C. Wang, G. Bosman, and S. S. Li, J. Appl. Phys., **79**, 1486 (1996).

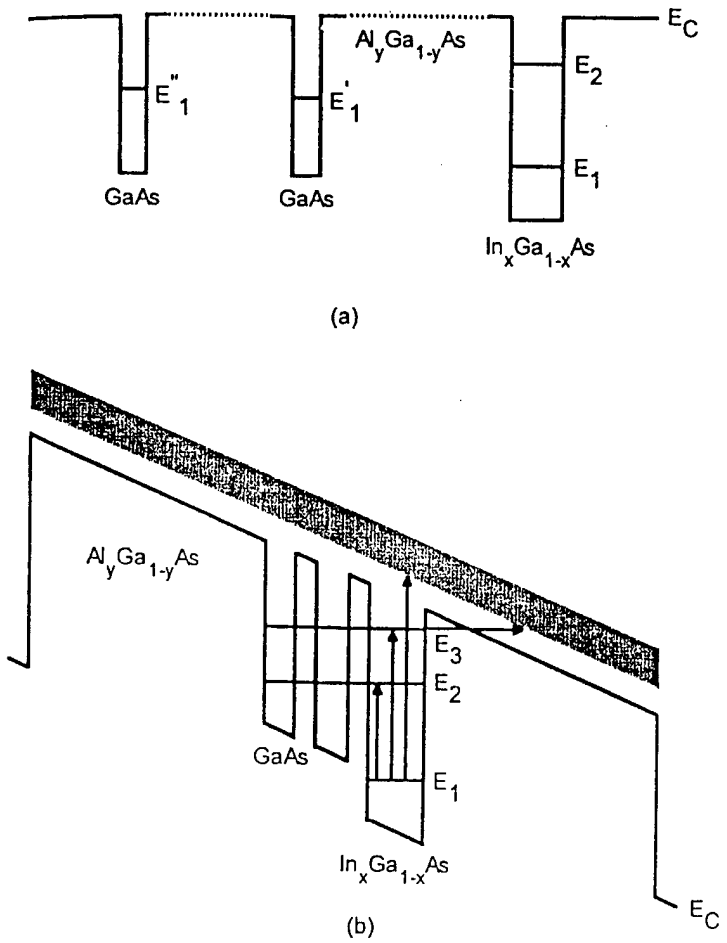

Figure 1. The schematic diagram of the conduction band and the bound state energy levels for (a) an isolated three QWs and for (b) a TC-QWIP under positive bias condition.

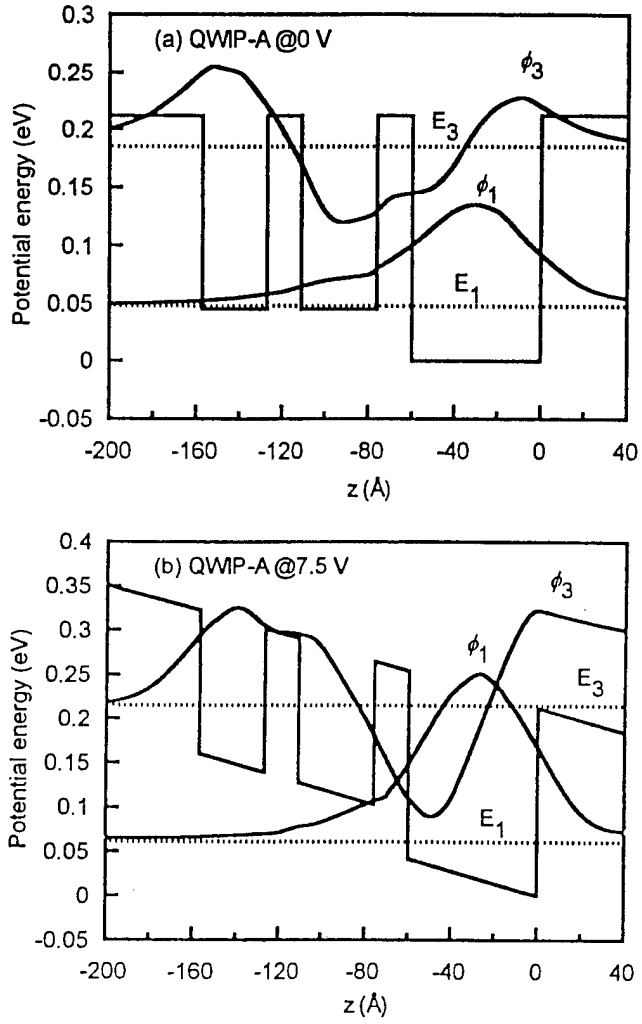

Figure 2. The calculated envelope wavefunctions of QWIP-A (a) under zero bias and (b) V_b = 7.5 V.

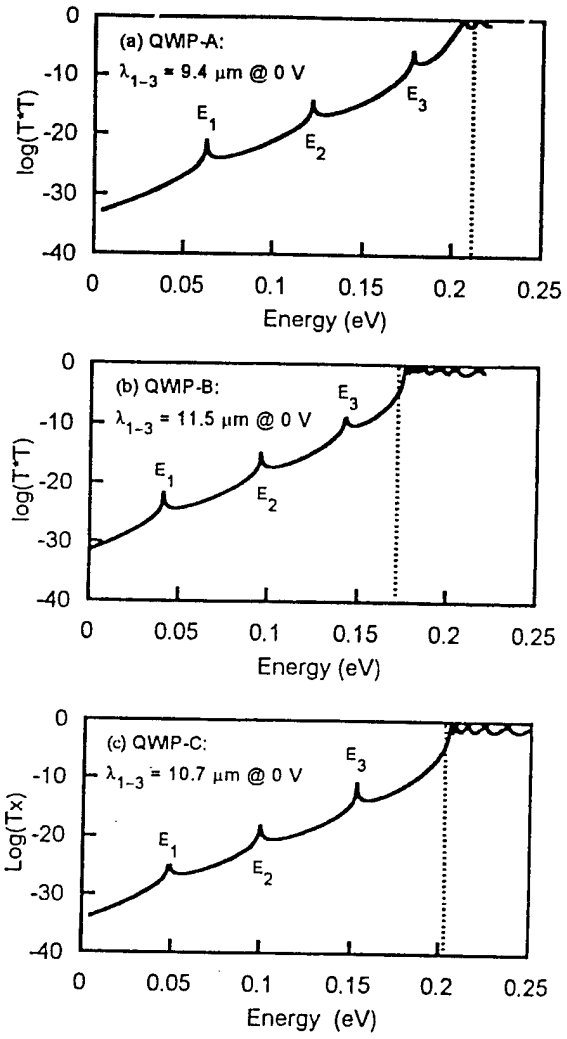

Figure 3. The calculated transmission coefficients of (a) QWIP-A, (b) QWIP-B, and (c) QWIP-C, respectively.

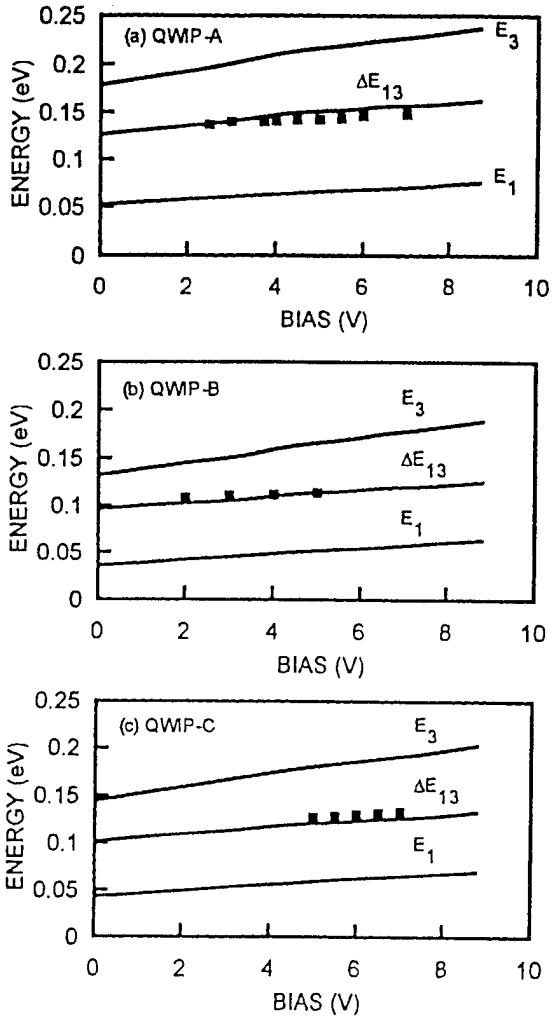

Figure 4. The calculated intersubband absorption energy and the subband energies as a function of the applied bias voltage for (a) QWIP-A, (b) QWIP-B, and (c) QWIP-C, respectively.

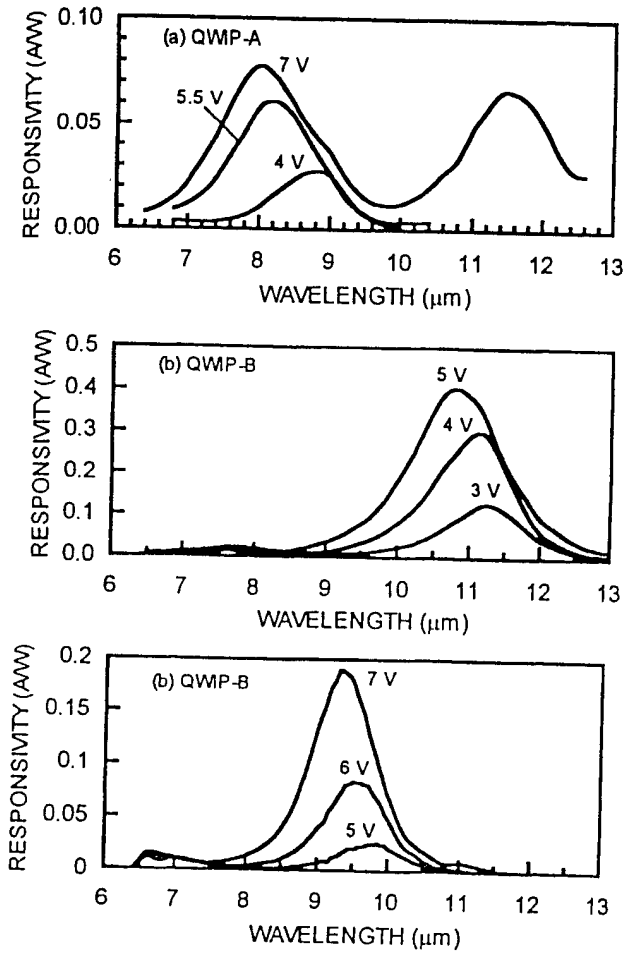

Figure 5. The spectral responsivity for (a) QWIP-A, (b) QWIP-B, and (c) QWIP-C, respectively.

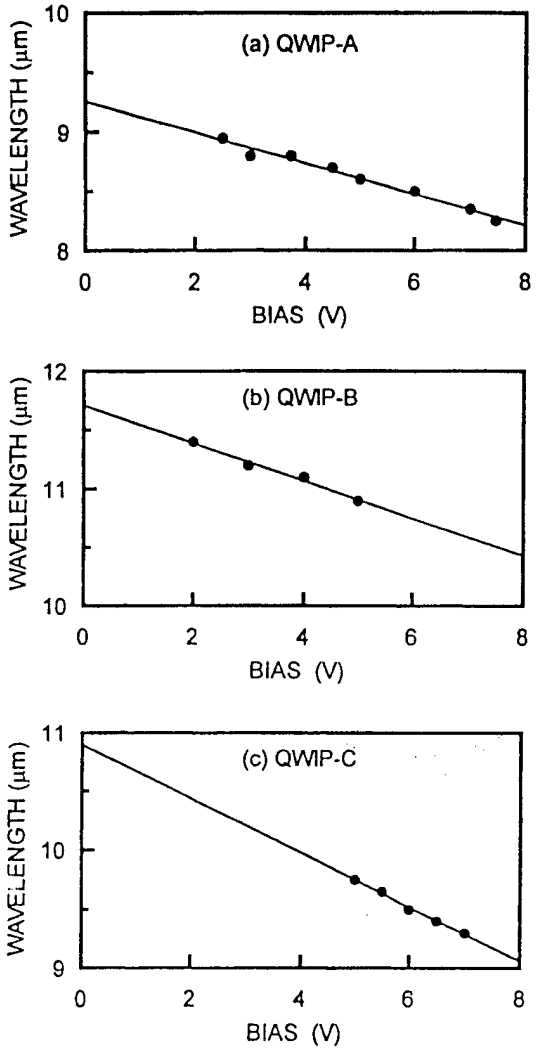

Figure 6. The wavelength tunabilities for (a) QWIP-A, (b) QWIP-B, and (c) QWIP-C, respectively.

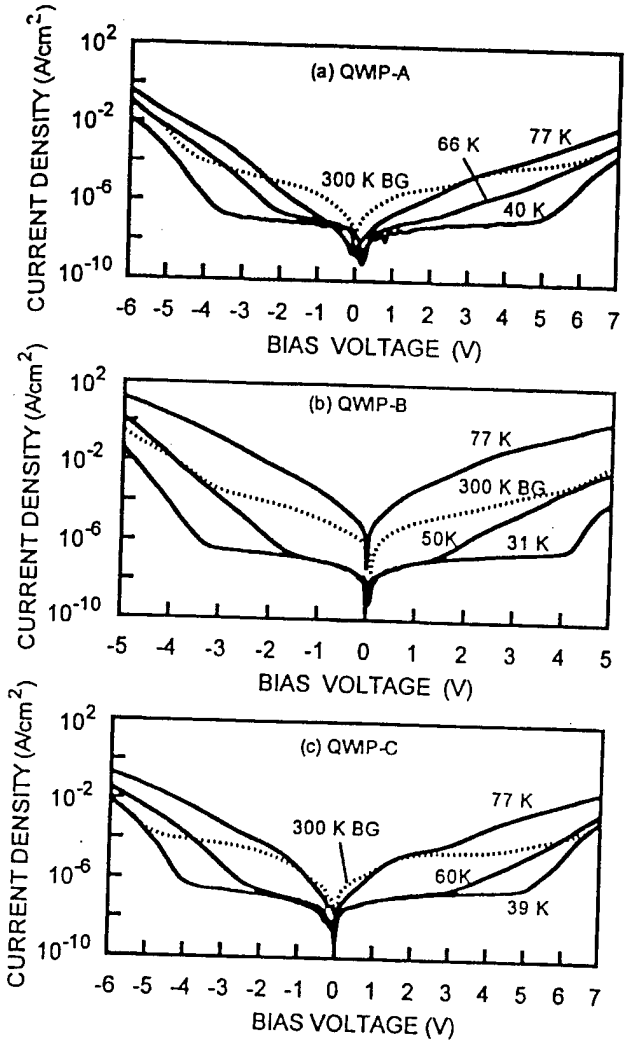

Figure 7. The dark *J-V* for (a) QWIP-A, (b) QWIP-B, and (c) QWIP-C, respectively.